Propulsion sizing correlations for electrical and fuel powered Unmanned Aerial Vehicles

Victor Alulema*, Esteban Valencia† , Edgar Cando‡, Victor Hidalgo§ and Dario Rodriguez¶
Escuela Politécnica Nacional, Quito, 170517, Ecuador

Despite the increasing demand of UAVs for a wide range of civil applications, there are few methodologies for their initial sizing. Nowadays, classical methods, mainly developed for transport aircraft, have been adapted to UAVs. However, these tools are not always suitable because they do not fully adapt to the plethora of geometrical and propulsive configurations that the UAV sector represents. Therefore, this work provides a series of correlations based on off-the-shelf components for the preliminary sizing of propulsion systems for UAVs. This study encompasses electric and fuel-powered propulsion systems, considering that they are the most used in the UAV industry and are the basis of novel architectures like hybrid propulsion. For these systems, weight correlations has been derived, and depending on data availability, correlations regarding their geometry and energy consumption are also provided. Furthermore, in order to highlight the implementation of the correlations a roadmap for conceptual and preliminary design stages is developed. To summarize,the main contribution of this work is to provide parametric tools to size rapidly the propulsion system components, which can be embedded on a UAV design and optimization framework. This research complements other correlation studies for UAVs, where the initial sizing of the vehicle is discussed. The present correlations suit multiple UAV categories ranging from micro to MALE UAVs.

I. Nomenclature

A	=	Regression coefficient
B	=	Regression coefficient
C	=	Cell o battery capacity
D	=	Diameter
FC	=	Fuel consumption
kV	=	Velocity constant of a brushless motor

*Research Engineer, Department of Mechanical Engineering / PIMI 15-03 Project
†Associate Professor, Department of Mechanical Engineering, AIAA Member
‡Associate Professor, Department of Mechanical Engineering
§Associate Professor, Department of Mechanical Engineering
¶Research Engineer, Department of Mechanical Engineering / PIMI 15-03 Project

L = Length

n = Number of observations in the database

P = Power

R^2 = Coefficient of correlation

T = Maximum static thrust

$TOGW$ = Take-off Gross Weight

$V_{nominal}$ = Nominal voltage

W = Mass of a propulsion system component

Subscripts

$cell$ = Elementary unit of a battery pack

EDF = Electric Ducted Fan

ICE = Internal Combustion Engine

jet = Turbojet engine

$motor$ = Electric brushless motor

$tprop$ = Turboprop engine

II. Introduction

At early stages of design, where the airplane layout is not well established yet, a large spectrum of aircraft configurations remains being a feasible design option. In this way, the large amount of architectures to be assessed at conceptual and preliminary design phases has encouraged the employment of parametric and semi-empirical models due to their rapid implementation and moderate computational cost while maintaining accurate results [1, 2]. In this sense, the conception of civil airplanes has historically relied on well documented parametric models, semi-empirical correlations and technical criteria, which has been derived from statistical data of operative aircraft [3–6]. Along the years, these correlations have been enhanced by including the recent advances on technology, which has enabled to assess non-conventional aircraft models (e.g. Blended Wing Body aircraft) [7, 8]. Furthermore, under certain considerations, these correlations have been firstly adapted and then employed for the conceptual design of unmanned aerial platforms that generally fit in the category of HALE UAVs [9–11]. However, their applicability on the design of other UAV categories (specially medium, small and micro) could lead to over or underestimate the aircraft components since UAVs employ different design trade-offs compared with transport aircraft [12].

In this context, the design of UAVs requires a personalized research to establish appropriate correlations that encompass the large spectrum of UAV categories. This could allow to size the different aircraft systems, like propulsion,

weight and geometry, in a more rapid and accurate way while considering the UAV's design requirements and performance constraints. In this sense, various authors have developed empirical correlations for conceptual and preliminary design based on statistical analysis of databases for different categories of UAVs [12–16]. These studies present several design charts and correlations that combines key parameters like wing loading and power loading as function of the payload mass or the vehicle's endurance. Therefore, these correlations enable to define other initial characteristics of the UAV such as power and thrust required, initial take-off mass, wing reference area, and rough estimates of the airplane dimensions. Regarding the sizing of UAVs' propulsion systems, Gur and Rosen [17] introduces several correlations for the energetic assessment and weight estimation of electric brushless motors and Li-Po batteries, while Ref [18] exhibits correlations for electrical sizing of brushless motors, electronic speed controllers, and batteries commonly used in multi-rotors. Although the aforesaid approaches are useful for small UAVs, they lack of data for larger vehicles and hence, they are biased to a small spectrum of UAV configurations. For instance, Ref. [18] limits the study of battery packs to 22.2 [V]. In similar fashion to electrical systems, there are few studies about the preliminary sizing of fuel engines focused on UAVs. In this way, Schoemann & Homung [19] provides a semi-empirical model to size piston engines for hybrid propulsion systems. However, their application involves a large number of engine parameters, most of them unknown at early design stages, which make them unsuitable for preliminary studies. In the other side, Ref. [20] exhibits correlations to estimate weight, size and specific power of ICE engines and turbine-based engines derived as power law functions; nevertheless, the range of power output varies from 10^2 to 10^5[KW], which make these correlations adequate for really large and heavy UAVs. With respect to turbine-based engines, these have been studied more deeply for civil aviation; for example, various correlations for weight estimation and their geometrical sizing can be found in Refs. [1, 3, 21]. Meanwhile, in ref. [22], the performance data of more than 1000 turbofan and turbojet engines have been compiled in an extended database for thrust values ranging from 10^4 to 5×10^6 [N]. Nonetheless, micro, small, and MALE UAVs employ power systems ranging lower than the aforesaid power and thrust ranges [9, 10, 23]. Thus, the above correlations and performance data can not be implemented to set the design space of smaller UAV configurations. In this study, the power output ranges from 10^{-1} to 10^2 [KW] and the thrust generated varies from 10^1 to 10^4 [N].

This work focuses on compiling a robust database of off-the-shelf components, covering a wide spectrum of UAV configurations, to enable the derivation of empirical correlations to size propulsion components at preliminary design stage. In this way, the commercial availability of these components can be accounted when optimization routines are implemented in the design of propulsion system. Hence, the importance of this work lies on complementing other correlations studies [12–20], since it can be embedded on UAV optimization and design routines to set preliminary aircraft parameters and determining their feasibility arranged in a certain configuration and based on market availability. This feature has been found of major importance in the optimal integration between airframe and propulsion systems for different UAV designs, since designers or hobbyist employ off-the-shelf components due to their low cost to set the

energy-propulsion configuration. Finally, Figure 1 shows the types of propulsion systems and the components that will be explored in this work. The proposed correlations are mainly focused on determining the preliminary weight and geometrical features of the propulsion components based on other UAV requirements regarding the mission planning stage.

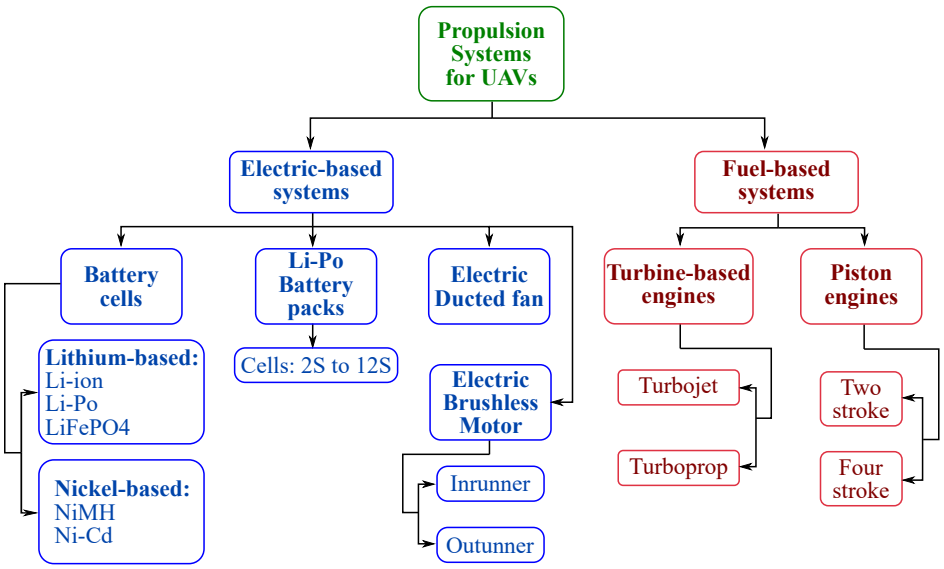

Fig. 1 Propulsion systems for UAVs addressed in this work

III. Methodology

The sizing correlations presented in this work are the result of a systematic data analysis based on the methodology presented in Refs. [14–16]. At the initial stage of this research, an extensive survey of different propulsion architectures for various vehicle configurations was carried out. These data revealed the existence of a wide spectrum of power plants for unmanned aircraft, ranging from fuel-based to electric-based propulsion [23–28]. For the components of the systems presented in Fig. 1, an exhaustive data gathering of off-the-shelf devices was developed in order to generate structured databases that integrate both design parameters and operational characteristics. The information used in the analysis was collected from state-of-art catalogues, online stores, and specialized forums. In order to ensure an accurate correlation, the dispersion of the data was constantly monitored through the Cook's distance criteria [29], which was employed to assess the influence of a specific observation in the regression analysis[30]. This principle allows to avoid deviations that affect the distribution of the parameters plotted along the range of study. The Cook's analysis was found very useful for the obtained correlations, since market trends and consumer preferences create a non-uniformly dispersed database, as observed in section IV.

The data analysis was performed in three sequential phases. Initially, the data sets were preliminary evaluated using techniques for classification and data visualization, following the approach described in ref. [30], where outlier and

leverage points are removed using the Cook's distance.

In order to describe the process of implementation of the correlations for preliminary sizing of UAV propulsion systems, a roadmap describing the variables and inputs required is depicted in Figure 2.

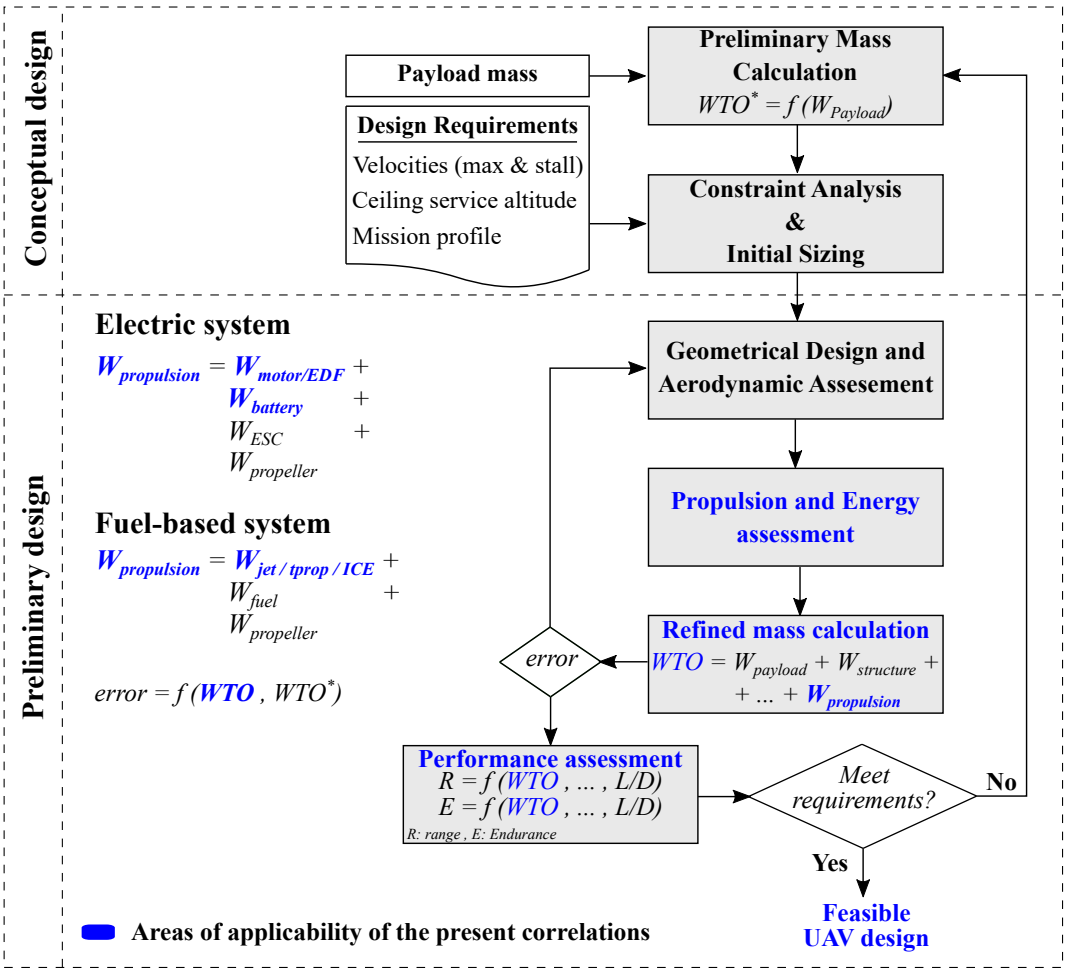

Fig. 2 Schematic roadmap for implementation of empirical correlations

As observed in figure 2 the geometrical and weight correlations (depicted in blue) enable prpulsion component sizing and since they are determined by using an extensive off-the-shelf database, they allow a refinement of the conceptual models and reduce the design space of potential solutions setting up their feasibility. This latter aspect is very important in preliminary design of UAVs, as the spectrum of UAVs architectures usually is very wide, making the determination of conceptual configurations cumbersome and unreliable if actual components are not considered.

IV. Results and discussion

This section compiles the correlations found for electric propulsion systems, which are based on ref. [30] and the correlations for fuel based propulsion systems.

A. Electric propulsion systems

As presented in Refs. [17, 18, 31], the main components of an electric propulsion system (conventional or hybrid-electric) are the electric motor, the electronic speed controller (ESC), the battery, and the propeller/fan. This section covers the formulation of sizing correlations for cells & batteries, electric ducted fans, and brushless motors (outrunner and inrunner). Propellers and ESCs have not been included in this analysis since information regarding these devices is widely available on the open domain * and their weight can be neglected when compared with batteries' or electric motors' weight [18].

1. Cells & Batteries

Batteries are the key components of electric propulsion systems since they supply the energy required to run the motor and other electric/electronic components for navigation, control and data acquisition [32]. The battery manages the performance of the UAV because it contributes significantly to the total weight of the UAV and plays an important role over the flight time (endurance), which depends directly on the battery capacity ($C_{battery}$) and UAV $TOGW$ [33]. For electric air vehicles, there are different battery types in terms of chemistry which are reported in the literature [28, 34, 35]. The electrical modelling, advantages and disadvantages of these devices are well reported in previous works [36–38] and hence, these topics were not explored in the present work. Instead, this section aims to present a sort of correlations for weight estimation of unitary cells and battery packs for the following battery chemistry: Li-Po, Li-ion, LiFePO4, NiCd, and NiMH.

In this study, three characteristics of cells & batteries are evaluated: capacity, voltage, and weight. In what respect to unitary cells, Fig. 3 illustrates the data collected from different manufacturers plotted in a logarithmic scale, meanwhile Table 1 presents the regression coefficients and the number of observations (n) in each data set. The database developed for this purpose includes: prismatic, flat, and cylindrical cells. It is important to mention that these data considers the wiring weight, envelope material and insulation covers. Moreover, as shown in Table 1, the coefficient R^2 shows good agreement with the data gathered (higher than 0.9 for all types of cell chemistry). The capacity of the unitary cell was selected as independent variable as it offers a direct link between the commercial selection of batteries and various performance characteristics such as endurance and range [33]. The range of capacity for each type of cell (internal composition) can be appreciated in Fig. 3, but in general, this study addressed battery cells from 30 [mAh] to 500 [Ah] of capacity. It is important to note that to make more generic the proposed correlations, the modeling has been defined for one cell, which then can be extrapolated for the case of larger number of cells. The present correlations intends to facilitate the studies over the performance of electric powered UAVs as a function of different characteristics from these power sources like battery internal composition, voltage (number of cells connected in-series) and capacity (number of cells connected in parallel).

*Technical info of propellers: `https://www.apcprop.com/technical-information/`
Performance data of propellers: `https://m-selig.ae.illinois.edu/props/propDB.html`

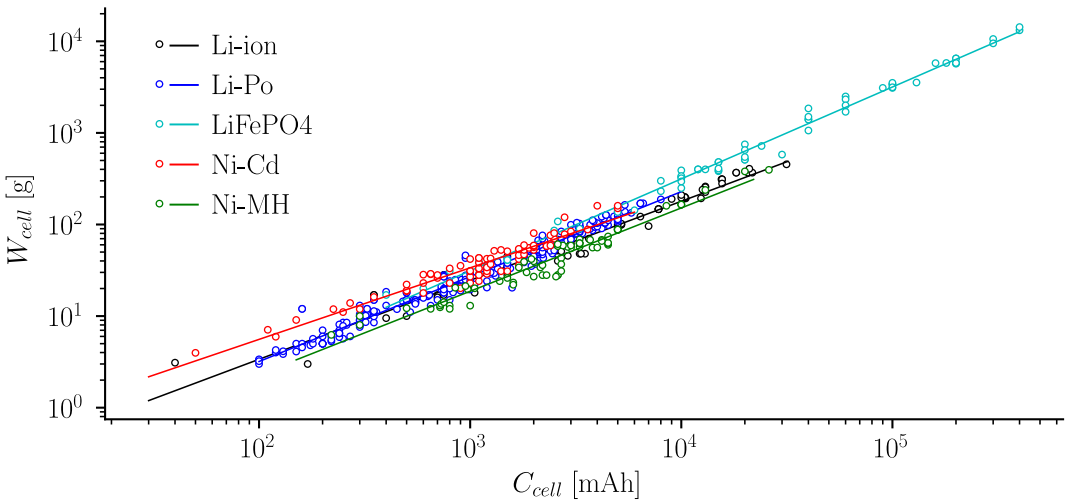

Fig. 3 Weight of unitary cells as function of cell capacity [30]

Table 1 Regression coefficients for unitary cells. $W_{cell} = A \cdot C_{cell}{}^{B}$ [30]

Type	A	B	R^2	n	$V_{nominal}$ $[V]$
Li-ion	0.0635	0.8627	0.9644	77	3.7
Li-Po	0.0446	0.9273	0.9696	241	3.7
LiFePo4	0.0306	1.0031	0.9918	64	3.3
Ni-Cd	0.1524	0.7813	0.9237	73	1.2
Ni-MH	0.0349	0.9095	0.9439	66	1.2

Since Li-Po cells and Li-Po batteries are the most utilized in micro, small and MALE commercial UAVs, they have been further studied to offer a better description for different cell arrangements. The data collected was plotted in two separate figures for facilitate their visualization and to divide the analysis in two main categories. On the one hand, Figure 4a groups Li-Po battery that are commonly used by RC (remote control) and FPV (First person view) micro and small UAVs, while batteries from Fig. 4b are most oriented to larger UAVs that requires higher values of power. Table 2 presents the regression coefficients obtained from the aforesaid plots and the number of observations for each number of battery cells. Analogously to the correlations previously presented, the coefficient R^2 shows a good capture of the data gathered.

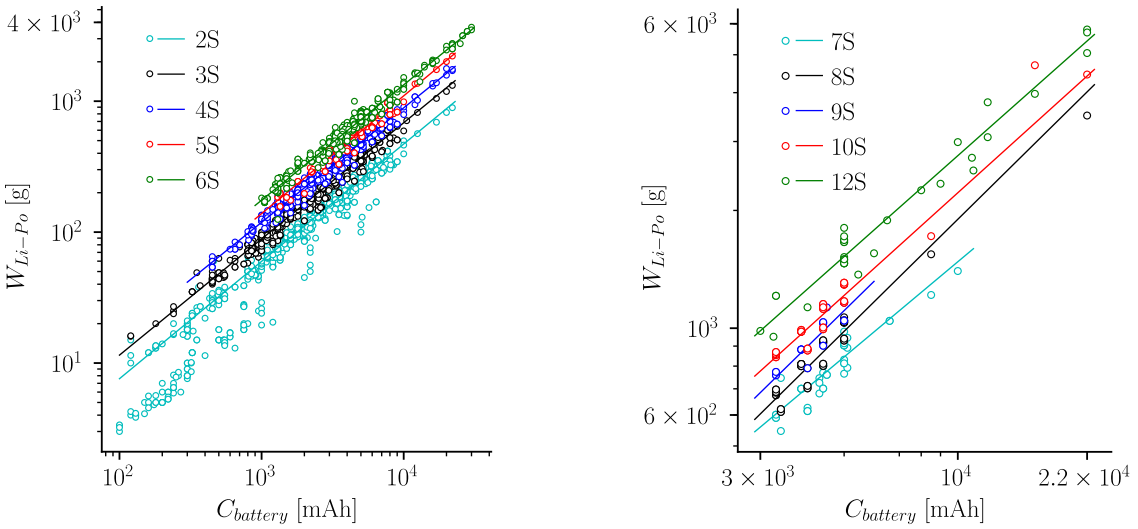

Fig. 4 Weight of Li-Po battery packs as function of battery capacity [30]

Table 2 Regression coefficients for Li-Po battery packs. $W_{Li-Po} = A \cdot C_{battery}^{B}$ [30]

N_{cells}	2S	3S	4S	5S	6S	7S	8S	9S	10S	12S
A	0.1224	0.1931	0.2828	0.2777	0.3988	0.8657	0.2975	0.3564	0.7246	1.0378
B	0.8963	0.8874	0.8744	0.8993	0.8810	0.8081	0.9512	0.9443	0.8715	0.8562
R^2	0.9723	0.9741	0.9763	0.9509	0.9761	0.8553	0.9527	0.8423	0.9434	0.9675
n	719	620	440	141	346	43	51	21	47	31

2. Electric ducted fan (EDF)

EDFs are propulsive components that generate thrust because of the pressure difference between the flow intake and exit station. Since these devices operate at high RPM, they also demand less torque compared with simple propellers while generating the same amount of thrust with less power. Moreover, the differences in performance of both propulsion systems has caused that EDFs are modeled in a different way [39]. Firstly, higher rotational speeds and lower torque demand the employment of brushless inrunner motors [40] unlike propellers that are commonly associated with outrunner motors. These assumptions have been taken into account when establishing the correlations that associate key preliminary characteristics of a EDF presented in this section. For this, compiled data from different sources[†] has resulted in a database of 270 ducted fan units from 12 different manufacturers that includes EDFs manufactured with plastic, aluminum, steel, and carbon-fiber parts. Considering that the function of an EDF is to generate thrust, the

[†]EDF by brand `https://www.turbines-rc.com/en/127-edf-by-brand`

maximum static thrust (provided by manufacturers) has been defined as the independent variable. This assumption was also used in Ref. [1], where correlations to determine the weight, diameter and length of large turbofan engines are presented. According to Refs. [39, 41, 42], the maximum static thrust specified by manufacturers can be assumed as the thrust required for take-off or can be calculated using the approaches presented in Refs. [39, 43].

Figure 5a introduces a correlation to determine the voltage constant (KV_{motor}) of a brushless inrunner motor as a function of the maximum static thrust, meanwhile Figure 5b provides a correlation to estimate the power that a battery must supply to an electric motor in order to generate a certain amount of thrust. On the other hand, Figure 5c present two correlations to determine the weight of the EDF from two different perspectives (Equations 1 and 2). The former Equation allows to calculate the weight of the EDF from the maximum static thrust that the fan generates, while in Equation 2, the EDF weight is estimated from the voltage constant of the electric motor, which implicitly involves the number of RPM of the fan and the voltage that is supplied to the electric motor. Finally, Figure 5d presents a correlation to size the duct diameter as function of the weight of the EDF. For all of the proposed models, the coefficient R^2 shows good match between the power law and the data collected. The gathered data also revealed some particular features of electric ducted fans. For instance, two EDFs of the same diameter and weight can generate different amounts of thrust depending on the KVs of the electric motor. Similarly, two EDFs powered by the same electric motor can generate similar values of thrust and weight differently depending on the diameter of the duct and the number of fan blades.

$$W_{EDF} = 24.116\, T^{\,0.8051} \quad , \quad R^2 = 0.8770 \tag{1}$$

$$W_{EDF} = 441839\, KV_{motor}^{-0.9571} \quad , \quad R^2 = 0.8225 \tag{2}$$

3. Electric brushless motors

Brushless motors are other key component in electric propulsion systems since they convert the electrical power stored in the battery into mechanical power [17, 18]. Refs. [40, 44, 45] describe thoroughly the electrical modelling and performance of such devices. However, for the preliminary design of electric-powered UAVs, general properties of the electric motor (e.g. weight, power, motor constant) are of greater interest. Refs. [17–19] present some correlations to determine the weight, diameter, no load current and internal resistance of the electric brushless motor; nevertheless, the accuracy of those correlations is questionable because of two factors: the really low value of the coefficient of correlation R^2 (where provided), and the number of data points and manufacturers included in those analysis. Similar to previous works [17–19], the motor constant (KV_{motor}) was defined as independent variable for this study, since it offers a direct link between the commercial selection of brushless motors and the number of RPM of the propeller and the voltage of the battery that powers the electric motor.

In order to determine highly accurate correlations, several approaches were evaluated in this work. The first

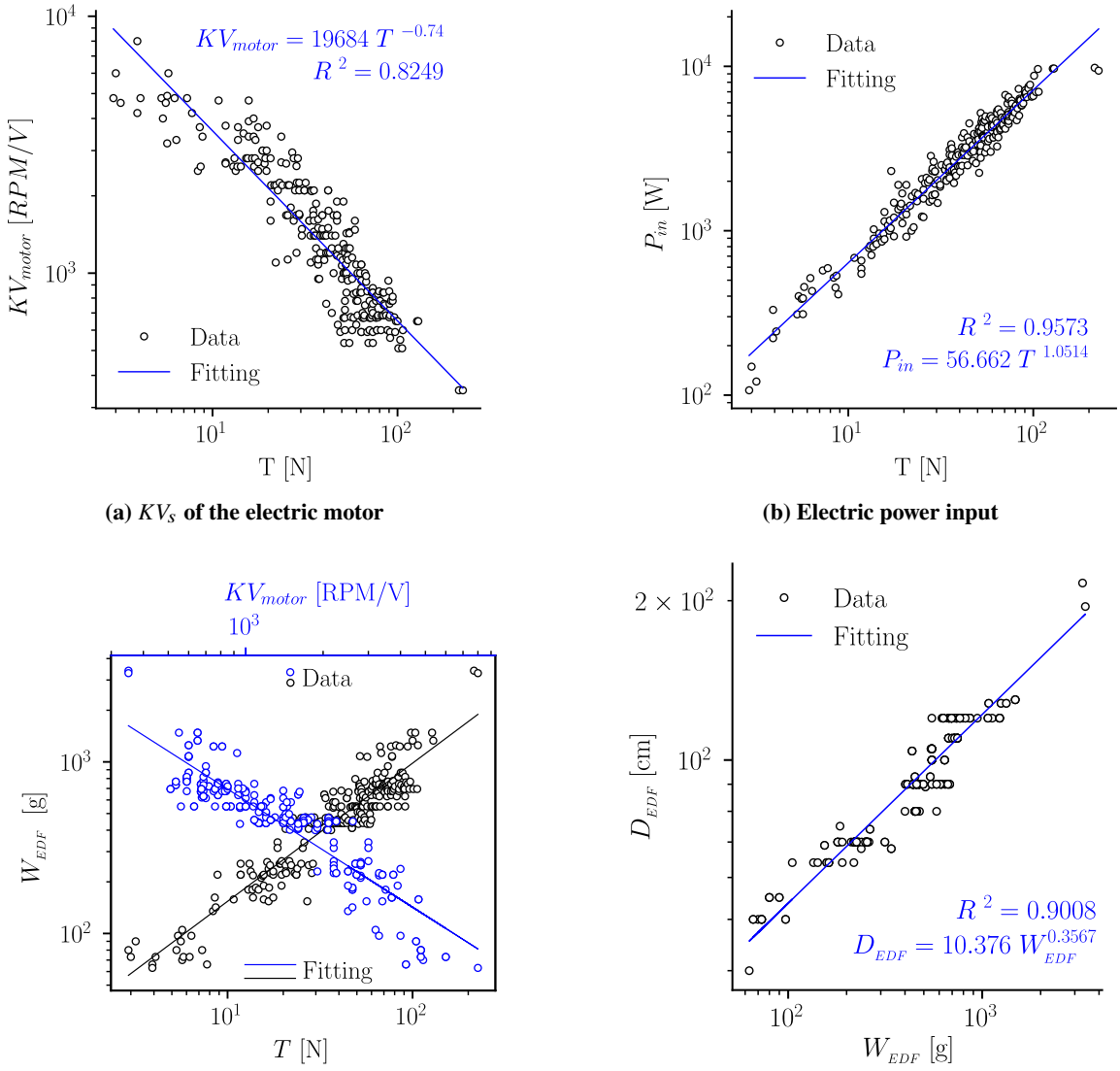

(a) KV_s of the electric motor

(b) Electric power input

(c) Weight of the EDF unit

(d) Diameter of the fan duct

Fig. 5 Sizing correlations for EDF from 2 up to 250 [N] of maximum static thrust. $n = 270$ [30]

approach was to establish a robust database that enables various statistical analysis. For this, data were collected from 12 manufacturers of outrunner motors and from 10 manufacturers of inrunner motors. Initially, a global correlation that encompasses the whole range of the motor constant was determined, nonetheless, the coefficient of correlation was lower than 0.5. Other approaches were to determine correlations for groups of manufacturers, segment the range of study, and vary the number of data points for the regression model. In fact, these approaches allowed to increase slightly the value of the coefficient of correlation; notwithstanding, the increase was not representative. Unlike batteries and EDFs, it was not possible to derive accurate correlations for brushless motors due to their non-linear behavior. This is reflected on the disparity and non-uniformity of the gathered data (Figure 6), which makes difficult to model this type of motors with uni-variate [17, 18] and even with multi-variate models [19].

Figures 6a and 6b illustrate the brushless motor weight as a function of the motor constant. It can be appreciated that these plots present an analogous behavior to the ones found in Refs. [17–19]. The number of magnetic poles of the motor was employed to split the aforesaid plots in different categories. As stated in Refs. [40, 45], the larger number of motor poles, the lower the motor constant. This behavior is clearly observed in Fig. 6 for both inrunner and outrunner motors. Even though no accurate correlations were determined, some trade-offs were identified. Table 3 presents a classification of electric brushless motors as function of the motor constant, four categories have been identified for both inrunner and outrunner motors. **Class I and II**: these categories group brushless motors for heavy duty applications, these motors provide really high values of torque and power at relatively low number of RPM. **Class III**: motors for small RC and FPV UAVs fall in this category, widely used for aero-modelling. These motors have intermediate values of torque and RPM. **Class IV**: this category comprises motors of low torque and high RPM, commonly used for small and micro UAVs.

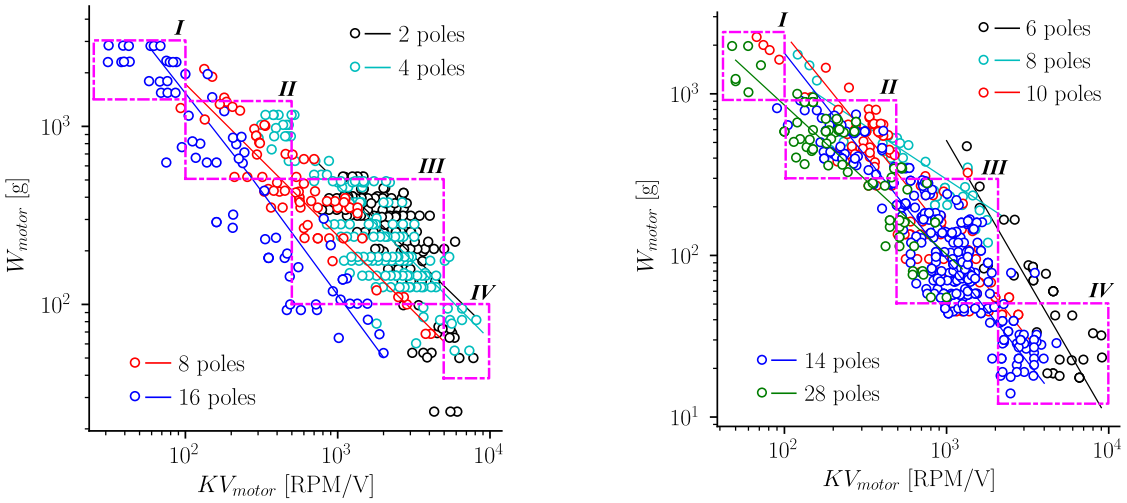

(a) Brushless INRUNNER motor. $n = 650$

(b) Brushless OUTRUNNER motor. $n = 750$

Fig. 6 KV_{motor} **and** W_{motor} **characteristics of electric brushless motors**

Table 3 Range of motor weight as function of KV_{motor}. (Based on Figure 6)

	Inrunner		Outrunner	
Class	KV_{motor}	W_{motor} [g]	KV_{motor}	W_{motor} [g]
I	50-100	1500-3000	50-100	9000-2500
II	100-500	500-1500	100-500	300-9000
III	500-5000	100-500	500-2000	50-300
IV	5000-10000	30-100	2000-10000	10-50

B. Fuel-based propulsion systems

Fuel-based propulsion systems, turbine-based and piston engines, are commonly employed on small, MALE and HALE UAVs because they permit to accomplish longer endurance and range [20, 25, 26]. The following section presents a group of correlations for sizing and selection of fuel-based engines focused on turbojet, turboprop, and internal combustion engines. Turbofan engines were not included in this study because very few devices for UAV applications were encountered.

1. Turbojet and turboprop engines

In this section, sizing correlations of turbojet and turboprop engines for UAV applications are presented. For this aim, a database consisting of 117 turbojet engines from 15 manufactures was structured and includes majorly single spool turbines and few double spool. In this case, the maximum static thrust was selected as independent variable, since the function of turbojet engines is to generate thrust from the high energy of the exit flow. On the other hand, the database for turboprop engines contains only 19 samples from 8 manufacturers. This type of engines are manufactured in lower quantity than other engine types due to their higher cost and complexity. For this case the power output has been used as independent variable, since turboprops are used to provide power shaft to the propulsive system. Both, the maximum static thrust and the power output are also employed by the manufacturers to characterize turbojet and turboprop engines, respectively. As mentioned in the section of EDFs, the maximum static thrust can be estimated using different approaches and assumptions, see section IV.A.2, while the rated power that manufacturers provide is the power output at cruise conditions, according to the manufacturers themselves.

For turbojet engines, correlations to estimate their weight, diameter, length and fuel consumption were derived. Figure 7 illustrates the data collected and, both the correlation and the R^2 coefficient are presented in each subplot. The weight of the turbojet engine (Figure 7a) does not include the weight of miscellaneous (e.g. fuel tank, additional air filters, etc). The diameter of the engine (Figure 7b) is the outer diameter and the length is measured from the inlet station to the end of the nozzle (Figure 7c). Most of manufacturers provide the fuel consumption in $[ml/min]$; therefore, it was preferred to maintain the units for this parameter (Figure 7d). Figure 8 present a correlation for weight estimation of turboprop engines as function of their power output. From the data collected, it was appreciated that most turboprop engines consist of a turbojet engine connected with a gearbox and a clutch. Thus, the correlations to determine the diameter and the fuel consumption of turbojet engines are also valid for turboprop ones. Finally, the regression coefficients show good fitting between the data collected and the power law model, R^2 higher than 0.9 for all the variables depicted.

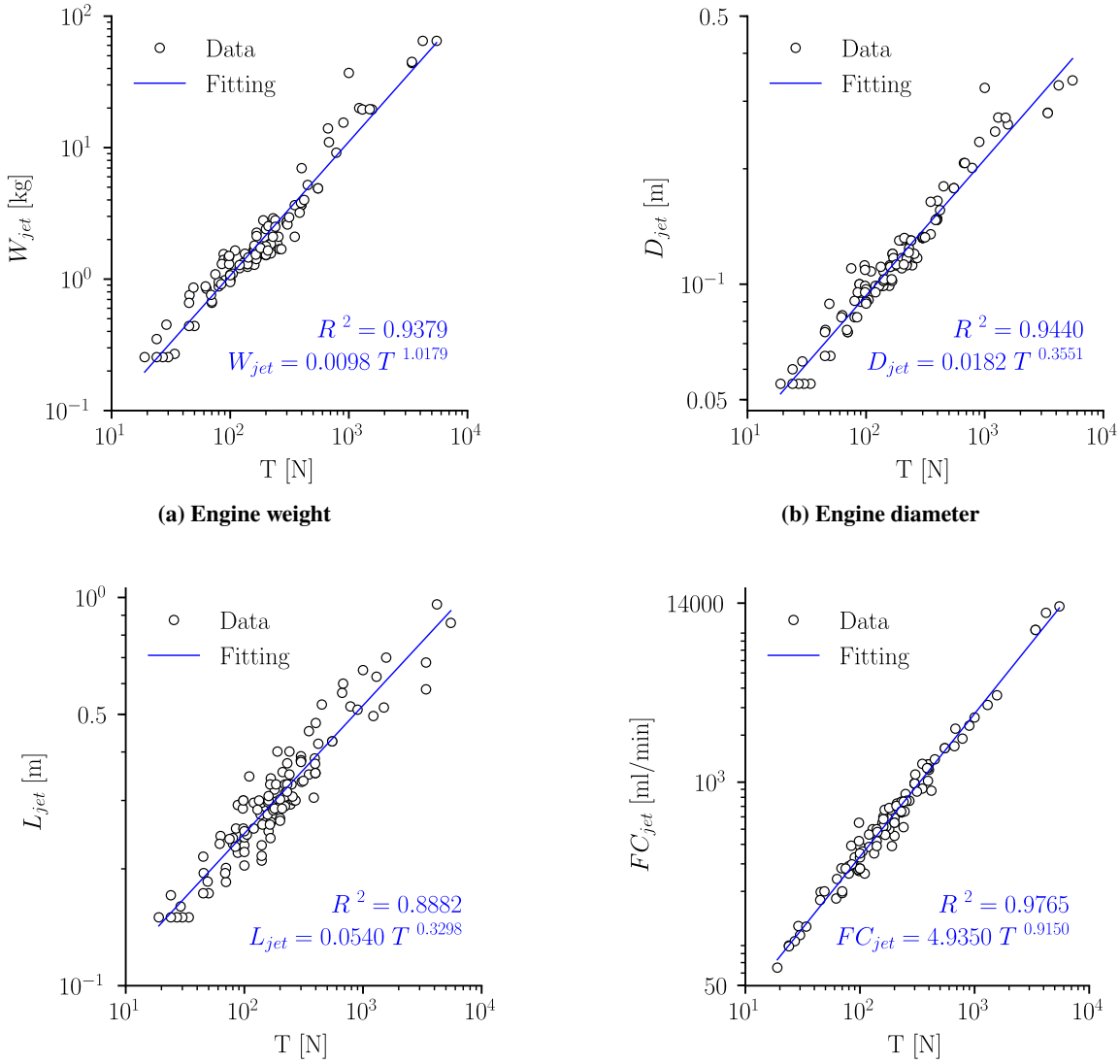

(a) Engine weight **(b) Engine diameter**

(c) Engine length **(d) Fuel consumption**

Fig. 7 Sizing correlations for turbojet engines from 20 up to 10000 [N] of maximum thrust

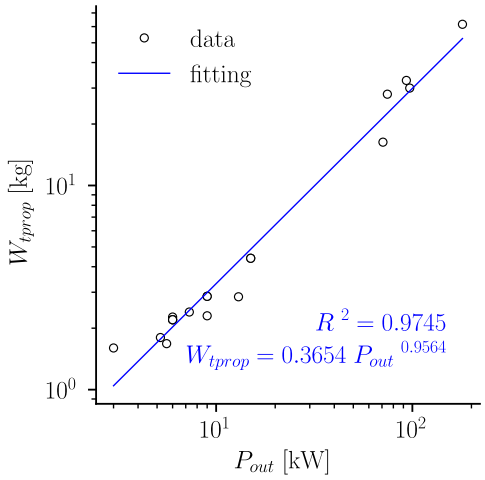

Fig. 8 Weight of turboprop engines from 2 up to 200 kW of cruise power. $n = 20$

2. Internal combustion engine

The low cost of these systems, compared with turbine-based engines, make them attractive for the small and MALE UAV sectors. The higher specific energy, compared with their electric counterparts, is also another reason for their use in long endurance unmanned aircraft. The thermodynamic modelling of these power machines is well documented [46, 47]; however, more general parameters of the engine (e.g. weight, displacement, power) are required at early stages of aircraft design. This section presents correlations to determine the weight and the displacement of two stroke and four stroke ICE engines. For this, a database based on off-the-shelf engines was assembled. The database cover engines from 35 manufacturers, including different configurations (e.g. single piston, V-type, Wankel) and various fuel types (e.g. regular gasoline, AVGAS, nitromethane). As a result, a total of 114 two stroke engines and 113 four stroke engines were surveyed. Afterwards, correlations to estimate engine's weight (Figure 9a and Table 4) and displacement (Figure 9b and Table 5) were derived as a function of the power output. These three parameters are used by manufacturers to characterize an ICE engine and are also useful for engine selection. The power output provided by the manufacturers is the power at cruise condition. From the data collected, it was identified two engine categories, which are marked in Figures 9a and 9b. Engines located in the white zone (left of the plot) can operate at moderate altitudes (< 3000 [masl]), while engines in the gray zone (right zone of the plot) have been optimized for operation at high altitudes (up to 5500 [masl] approx.). In similar fashion to previous power systems, the coefficient of correlation shows a good match between the data collected and the power law model, which has enabled to define simple but accurate correlations to size ICE engines.

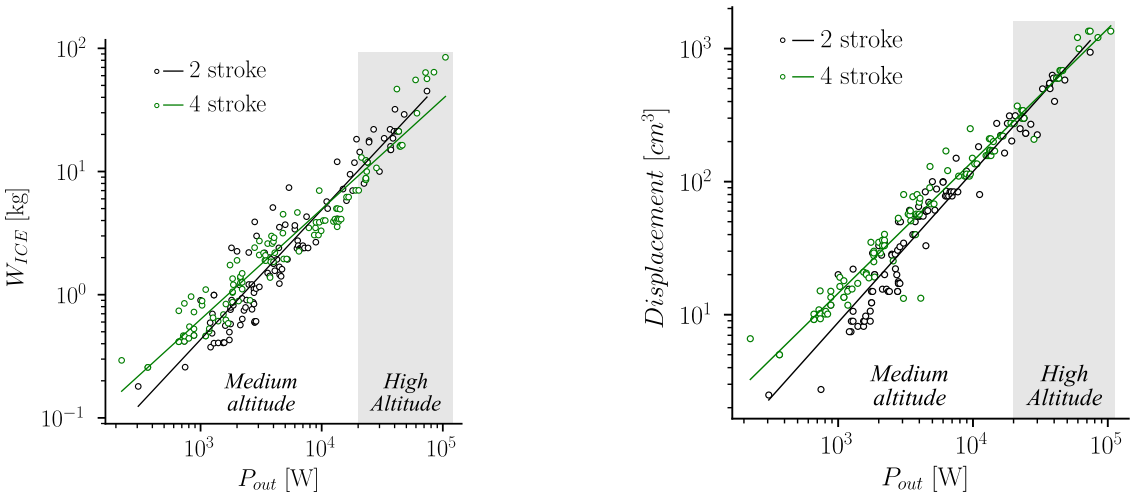

(a) Engine weight **(b) Displacement**

Fig. 9 Sizing correlations for ICE engines from 200 up to 100000 W of cruise power

Table 4 Weight of ICE engines, regression coefficients. $W_{ICE} = A \cdot P_{out}^{B}$

	A	B	R^2	n
Two stroke	0.0003	1.0530	0.8959	114
Four stroke	0.0013	0.8952	0.9300	113

Table 5 Displacement of ICE engines, regression coefficients. $Displacement = A \cdot P_{out}^{B}$

	A	B	R^2	n
Two stroke	0.0035	1.1327	0.9353	114
Four stroke	0.0151	0.9940	0.9612	113

V. Conclusions

A series of correlations for sizing the UAV's propulsion systems were developed based on off-the shelf components. Although the proposed correlations covers a large spectrum of UAVs, a greater emphasis was placed on vehicles ranging from micro to MALE. For the development of these models, the Cook's distance criteria was employed to reduce the dispersed data and then, statistical analysis was performed to derive the sizing correlations following a power law. The results obtained showed good agreement and satisfactory correlations indexes, which make them suitable for conceptual and preliminary design phases. The main contribution of this work lies on fulfillment of the gap in the broad spectrum of design alternatives that UAVs represent, where current models do not provide a scheme for assessing the feasibility of

the propulsion configurations when using off-the-shelf components. This aspect makes the present work a useful tool to be implemented in any optimization routine for defining weight and main geometrical features of a propulsion system, accelerating the design process at early stages.

VI. Acknowledgements

The authors gratefully acknowledge the financial support provided by Escuela Politécnica Nacional for the development of the projects: PIMI 15-03, PIMI 18-01, PIJ 15-11 and PIS 16-20. Furthermore, the authors thank the support of CEDIA through the project CEPRA 12-XII-2018.

References

[1] Isikveren, A. T., "Quasi-analytical modelling and optimisation techniques for transport aircraft design," Ph.D. thesis, Royal Institute of Technology (KTH), 2002.

[2] Chambers, M. C., Ardema, M. D., Patron, A. P., Hahn, A. S., Miura, H., and Moore, M. D., "Analytical fuselage and wing weight estimation of transport aircraft," 1996.

[3] Torenbeek, E., *Synthesis of subsonic airplane design: an introduction to the preliminary design of subsonic general aviation and transport aircraft, with emphasis on layout, aerodynamic design, propulsion and performance*, Springer Science & Business Media, 1982.

[4] Roskam, J., *Airplane design*, DARcorporation, 1985.

[5] Anderson, J. D., *Aircraft performance and design*, Vol. 1, WCB/McGraw-Hill Boston, MA, 1999.

[6] Nield, B. N., "An overview of the Boeing 777 high lift aerodynamic design," *The Aeronautical Journal*, Vol. 99, No. 989, 1995, pp. 361–371.

[7] Liebeck, R., Page, M., and Rawdon, B., "Blended-wing-body subsonic commercial transport," *36th AIAA Aerospace Sciences Meeting and Exhibit*, 1998, p. 438.

[8] Torenbeek, E., *Advanced aircraft design: conceptual design, analysis and optimization of subsonic civil airplanes*, John Wiley & Sons, 2013.

[9] Bravo-Mosquera, P. D., Cerón-Muñoz, H. D., Díaz-Vázquez, G., and Catalano, F. M., "Conceptual design and CFD analysis of a new prototype of agricultural aircraft," *Aerospace Science and Technology*, Vol. 80, 2018, pp. 156–176.

[10] Panagiotou, P., Kaparos, P., Salpingidou, C., and Yakinthos, K., "Aerodynamic design of a MALE UAV," *Aerospace Science and Technology*, Vol. 50, 2016, pp. 127–138.

[11] Kontogiannis, S. G., and Ekaterinaris, J. A., "Design, performance evaluation and optimization of a UAV," *Aerospace science and technology*, Vol. 29, No. 1, 2013, pp. 339–350.

[12] Sóbester, A., Keane, A., Scanlan, J., and Bressloff, N., "Conceptual design of UAV airframes using a generic geometry service," *Infotech@ Aerospace*, 2005, p. 7079.

[13] Gundlach, J., *Designing unmanned aircraft systems: a comprehensive approach*, American Institute of Aeronautics and Astronautics, 2012.

[14] Götten, F., Finger, D., Braun, C., Havermann, M., Bil, C., and Gómez, F., "Empirical correlations for geometry build-up of fixed wing unmanned air vehicles," *Asia-Pacific International Symposium on Aerospace Technology*, Springer, 2018, pp. 1365–1381.

[15] Verstraete, D., Palmer, J. L., and Hornung, M., "Preliminary Sizing Correlations for Fixed-Wing Unmanned Aerial Vehicle Characteristics," *Journal of Aircraft*, Vol. 55, No. 2, 2017, pp. 715–726.

[16] Gómez-Rodríguez, Á., Sanchez-Carmona, A., García-Hernández, L., and Cuerno-Rejado, C., "Preliminary Correlations for Remotely Piloted Aircraft Systems Sizing," *Aerospace*, Vol. 5, No. 1, 2018, p. 5.

[17] Gur, O., and Rosen, A., "Optimizing electric propulsion systems for unmanned aerial vehicles," *Journal of aircraft*, Vol. 46, No. 4, 2009, pp. 1340–1353.

[18] Bershadsky, D., Haviland, S., and Johnson, E. N., "Electric multirotor UAV propulsion system sizing for performance prediction and design optimization," *57th AIAA/ASCE/AHS/ASC Structures, Structural Dynamics, and Materials Conference*, 2016, p. 0581.

[19] Schoemann, J., and Hornung, M., "Modeling of hybrid electric propulsion systems for small unmanned aerial vehicles," *12th AIAA Aviation Technology, Integration, and Operations (ATIO) Conference and 14th AIAA/ISSMO Multidisciplinary Analysis and Optimization Conference*, 2012, p. 5610.

[20] Cirigliano, D., Frisch, A. M., Liu, F., and Sirignano, W. A., "Diesel, spark-ignition, and turboprop engines for long-duration unmanned air flights," *Journal of Propulsion and Power*, Vol. 34, No. 4, 2017, pp. 878–892.

[21] Mattingly, J. D., Heiser, W. H., and Pratt, D. T., *Aircraft engine design*, American Institute of Aeronautics and Astronautics, 2002.

[22] Roux, E., *Turbofan and turbojet engines: database handbook*, Elodie Roux, 2007.

[23] Lidor, A., Weihs, D., and Sher, E., "Novel Propulsion Systems for Micro Aerial Vehicles," *Journal of Propulsion and Power*, Vol. 35, No. 1, 2018, pp. 243–267.

[24] Griffis, C. L., Wilson, T. A., Schneider, J. A., and Pierpont, P. S., "Framework for the conceptual decomposition of unmanned aircraft propulsion systems," *Aerospace Conference, 2008 IEEE*, IEEE, 2008, pp. 1–10.

[25] Griffis, C., Wilson, T., Schneider, J., and Pierpont, P., "Unmanned Aircraft System Propulsion Systems Technology Survey," *Embry Riddle, Scholarly commons*, 2009.

[26] Gupta, S. G., Ghonge, M. M., and Jawandhiya, P., "Review of unmanned aircraft system (UAS)," *International Journal of Advanced Research in Computer Engineering & Technology (IJARCET)*, Vol. 2, No. 4, 2013, pp. pp–1646.

[27] Adamski, M., "Analysis of propulsion systems of unmanned aerial vehicles," *Journal of Marine Engineering & Technology*, Vol. 16, No. 4, 2017, pp. 291–297.

[28] Cwojdziński, L., and Adamski, M., "Power units and power supply systems in UAV," *Aviation*, Vol. 18, No. 1, 2014, pp. 1–8.

[29] Huitema, B., *The analysis of covariance and alternatives: Statistical methods for experiments, quasi-experiments, and single-case studies*, Vol. 608, John Wiley & Sons, 2011.

[30] Alulema, e. a., Victor, "Preliminary sizing correlations for UAVs' propulsion system," *AIAAPropulsion and Energy forum 2019*, 2019, p. 10.

[31] Logan, M., Chu, J., Motter, M., Carter, D., Ol, M., and Zeune, C., "Small UAV research and evolution in long endurance electric powered vehicles," *AIAA Infotech@ Aerospace 2007 conference and exhibit*, 2007, p. 2730.

[32] Gong, A., and Verstraete, D., "Role of battery in a hybrid electrical fuel cell UAV propulsion system," *52nd AIAA Aerospace Sciences Meeting*, 2014.

[33] Traub, L. W., "Range and endurance estimates for battery-powered aircraft," *Journal of Aircraft*, Vol. 48, No. 2, 2011, pp. 703–707.

[34] Karunarathne, L., Economou, J. T., and Knowles, K., "Model based power and energy management system for PEM fuel cell/Li-Ion battery driven propulsion system," 2010.

[35] Jung, S., and Jeong, H., "Extended kalman filter-based state of charge and state of power estimation algorithm for unmanned aerial vehicle Li-Po battery packs," *Energies*, Vol. 10, No. 8, 2017, p. 1237.

[36] Crompton, T. P., *Battery reference book*, Elsevier, 2000.

[37] Fotouhi, A., Auger, D. J., Propp, K., Longo, S., and Wild, M., "A review on electric vehicle battery modelling: From Lithium-ion toward Lithium–Sulphur," *Renewable and Sustainable Energy Reviews*, Vol. 56, 2016, pp. 1008–1021.

[38] Kuhn, E., Forgez, C., Lagonotte, P., and Friedrich, G., "Modelling Ni-mH battery using Cauer and Foster structures," *Journal of power sources*, Vol. 158, No. 2, 2006, pp. 1490–1497.

[39] Marc de Piolenc, G. W., *Ducted fan design*, Mass Flow, 2001.

[40] Xia, C.-l., *Permanent magnet brushless DC motor drives and controls*, John Wiley & Sons, 2012.

[41] Sforza, P. M., *Commercial airplane design principles*, Elsevier, 2014.

[42] Mair, W. A., and Birdsall, D. L., *Aircraft performance*, Vol. 5, Cambridge University Press, 1996.

[43] Gudmundsson, S., *General aviation aircraft design: Applied Methods and Procedures*, Butterworth-Heinemann, 2013.

[44] Zeraoulia, M., Benbouzid, M. E. H., and Diallo, D., "Electric motor drive selection issues for HEV propulsion systems: A comparative study," *IEEE Transactions on Vehicular technology*, Vol. 55, No. 6, 2006, pp. 1756–1764.

[45] Hendershot, J. R., and Miller, T. J. E., *Design of brushless permanent-magnet machines*, Motor Design Books, 2010.

[46] Guzzella, L., and Onder, C., *Introduction to modeling and control of internal combustion engine systems*, Springer Science & Business Media, 2009.

[47] Taylor, C. F., *The Internal-combustion Engine in Theory and Practice: Combustion, fuels, materials, design*, Vol. 2, MIT press, 1985.